

Report Title	COHO - Utilizing Waste Heat and Carbon Dioxide at Power Plants for Water Treatment
Type of Report (Final Scientific/Technical or Topical)	Final Report
Reporting Period Start Date	10/1/2014
Reporting Period End Date	09/30/2016
Principal Author(s)	Sumanjeet Kaur, Aaron Wilson, Daniel Wendt, Jeffrey Mendelssohn, Olgica Bakajin, Erik Desormeaux, and Jennifer Klare
Date Report was Issued	July 25th, 2017
DOE Award Number and if appropriate, task number	DE-FE0024057
Name and Address of Submitting Organization	Porifera Inc. 3502 Breakwater Ct. Hayward, CA 94704

"This report was prepared as an account of work sponsored by an agency of the United States Government. Neither the United States Government nor any agency thereof, nor any of their employees, makes any warranty, express or implied, or assumes any legal liability or responsibility for the accuracy, completeness, or usefulness of any information, apparatus, product, or process disclosed, or represents that its use would not infringe privately owned rights. Reference herein to any specific commercial product, process, or service by trade name, trademark, manufacturer, or otherwise does not necessarily constitute or imply its endorsement, recommendation, or favoring by the United States Government or any agency thereof. The views and opinions of authors expressed herein do not necessarily state or reflect those of the United States Government or any agency thereof."

Abstract

The COHO is a breakthrough water purification system that can concentrate challenging feed waters using carbon dioxide and low-grade heat. For this project, we studied feeds in a lab-scale system to simulate COHO's potential to operate at coal-powered power plants. COHO proved successful at concentrating the highly scaling and challenging wastewaters derived from a power plant's cooling towers and flue gas desulfurization units. We also found that COHO was successful at scrubbing carbon dioxide from flue gas mixtures. Thermal regeneration of the switchable polarity solvent forward osmosis draw solution ended up requiring higher temperatures than initially anticipated, but we also found that the draw solution could be polished via reverse osmosis. A techno-economic analysis indicates that installation of a COHO at a power plant for wastewater treatment would result in significant savings.

Table of Contents

Abstract	3
EXECUTIVE SUMMARY	4
Acronym Table	5
1. Introduction	5
2. Accomplishments	8
3. Conclusion	39
4. Recommended Next Steps	40
5. References.....	41

EXECUTIVE SUMMARY

Zero Liquid Discharge (ZLD) wastewater treatment systems that reuse and treat all power plant process waters are increasingly necessary to meet tighter regulatory requirements. However, the treatment and reuse steps required to achieve Zero Liquid Discharge remains an expensive and energy intensive process. While some power plant wastewater can be easily treated for reuse within the plant, economically viable treatment of other wastewaters—such as Cooling Tower (CT) and Flue Gas Desulphurization (FGD) blow down wastewaters—remain elusive.

For this project, we tested operating our COHO water purification system against simulated CT blow down and FGD feed waters, and demonstrated COHO's ability to both produce clean water from these challenging feeds, while sequestering carbon dioxide (CO_2). We initially found that while the CT and FGD feed waters were problematic to treat, the addition of commercial antiscalants resulted in the successful concentration of the feed waters. We also found that COHO effectively removed all the CO_2 from simulated flue gas by reaction with the switchable polarity solute. This means that COHO can reduce CO_2 emissions from power plants and use CO_2 to power the COHO water purification system. The carbon dioxide from the system may also be sequestered for storage after use. A techno-economic analysis based on the experimental data from this project including capital and operational costs indicates that the total all-inclusive cost of COHO is \$3.24 per m^3 of FGD wastewater treated. This represents a 38% savings over state-of-the-art technologies and more than 50% savings over conventional evaporator systems.

Acronym Table

Capital Expense	CAPEX
Carbon Dioxide	CO ₂
COHO	CO ₂ -H ₂ O
Cooling Tower	CT
Forward Osmosis	FO
Flue Gas Desulfurization	FGD
Idaho National Laboratory	INL
Inside Battery Limits	ISBL
Liters/Meters ² /Hour	LMH
Mechanical Vapor Recompression	MVR
Multieffect Distillation	MED
Multistage Evaporators	MSE
Operating Expense	OPEX
Outside Battery Limits	OSBL
Reverse Osmosis	RO
Reverse Solute Flux	RSF
Switchable Polarity Solvent	SPS
Total Dissolved Solids	TDS
Total Suspended Solids	TSS
Zero Liquid Discharge	ZLD

1. Introduction

Forward osmosis (FO) has the potential to efficiently treat challenging wastewater containing high total suspended solids (TSS) and/or high total dissolved solids (TDS). In FO, two solutions of different salinity are brought into contact by a semi-permeable membrane [1-3]. This membrane allows the solvent (i.e. water) to

permeate and retains the solute (i.e. dissolved salts). One of the significant benefits of FO is that mass transport (i.e. water flux) across the membrane is driven by osmotic forces, not by mechanically applied pressure. FO enables the filtration of difficult-to-treat wastewater [4] without detrimental fouling.

A limitation on the use of FO for treatment of high TDS and/or TSS waters is the inadequate performance of available FO draws. Most FO draw solutions studied by researchers are inorganic salts (NaCl or MgCl_2) [5]. The use of salt limits the maximum obtainable osmotic pressure to the solubility of the salt. While sodium chloride can achieve a maximum osmotic pressure of 12.3 Osm/kg, osmotic pressures that most salts can achieve are significantly lower. In addition, at high salinity reverse osmosis (RO) is not feasible because it requires extremely high operating pressures. High operating pressures also severely limit percent water recovery in RO systems. Treatment of high TDS water requires a “designer” draw that can achieve extremely high osmotic pressures (~300 bar) and be easily removed. Idaho National Laboratory (INL) [6] developed a novel switchable draw based on switchable polarity solvents (SPS). The SPS draw, combined with FO, not only can treat challenging wastewater, but it also utilizes and captures CO_2 for sequestration. Also, thermal removal of the SPS draw solute via non-utilized low-grade waste heat derived from the power plant results in significant savings in energy costs when compared to traditional evaporative technologies. This SPS FO-based process, herein called COHO ($\text{CO}_2\text{-H}_2\text{O}$), is uniquely suited for power plants in its ability to capture carbon dioxide from the plant’s flue gas and use it to drive on-site treatment of the plant’s wastewater for reuse.

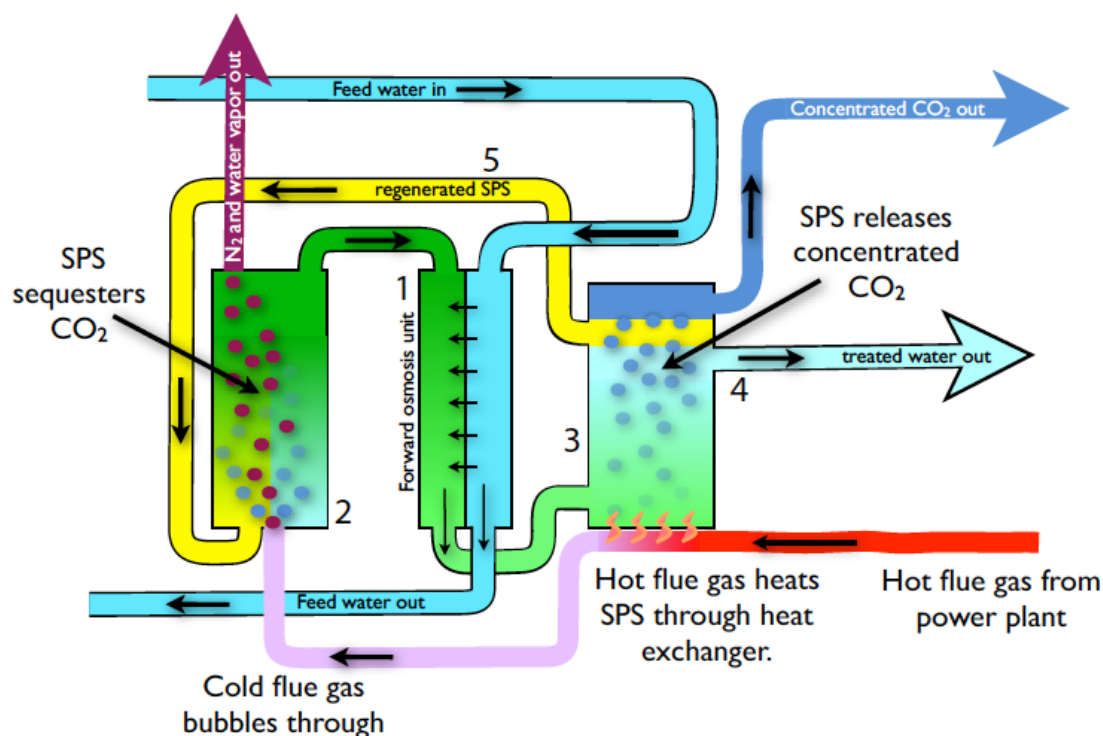


Figure 1. Schematic of COHO draw phase switching.

The process of draw phase switching by carbon dioxide is illustrated in Figure 1. The draw solution purifies wastewater by (1) using osmotic potential to drive water across a selective membrane and (2) generating draw solution by using carbon dioxide from flue gas to switch the draw solute to the miscible aqueous phase. Carbon dioxide is released (3) and clean water is produced (4) by using waste heat from the power plant, switching the draw solute (5) back to its original immiscible phase for mechanical separation. The SPS class of solvents is tertiary amines that switch between a non-ionic (aprotic) to a water-soluble ionic form in the presence of CO₂. The draw solute, dimethylcyclohexylamine, is a tertiary amine. It behaves as an SPS [7], and transitions from water miscibility (60 wt%) to water immiscibility (2000 ppm or less) depending on the presence or absence of carbon dioxide. Conventional FO systems with salt draws act primarily as a method for

pretreatment, homogenizing a water stream for ultimate purification through RO. The COHO system is significantly different; polarity switching is the critical event for the purification process. Once the draw solution has reached a desired dilution, the carbon dioxide is removed from the solution, driving a shift in the draw to its non-polar immiscible form, which then phase separates from the water. The two phases can then be mechanically separated. This draw has key characteristics of high osmotic pressures and a facile separation method.

The COHO will not only synergistically capture carbon dioxide and treat wastewater at power plants but also it will have higher recovery and lower energy costs compared to state-of-the-art technology. These advantages are essential in Zero Liquid Discharge (ZLD) power plants that reuse and treat all water on-site, currently an expensive (high capital costs) and energy intensive processes (high operating costs). Despite the high costs, ZLD power plants are increasingly necessary to meet tighter regulatory requirements regarding water intake, discharge, and greenhouse gas emissions. While some of the wastewater generated from the power plant can be easily treated for reuse within the plant, such as cooling tower (CT) blow down, other wastewaters like Flue Gas Desulphurization (FGD) blow down are more difficult to treat. For this project, we tested our COHO system with simulated CT and FGD waste waters, and demonstrated the abilities of COHO to both produce clean water from these challenge feeds and to capture CO₂.

2. Accomplishments

Process Optimization.

– Survey Typical Water Feeds.

Waste water processing is a technology where costs and methods must be tailored to

the requirements of a specific application. To understand the requirements for power plant water processing, we performed a search to find example feeds on which to base our experimental testing. While a literature search had few results, we were able to find information on the Merrimack Station plant, a large 440 MW coal burning power plant in New Hampshire commissioned in 1960. In 2011 the plant installed scrubbers and FGD units to improve air quality. In addition, Aquatech installed a ZLD unit to treat the FGD produced water. The water quality data is shown below in Table 1.

Table 1. Merrimack Station Coal Power FGD Wastewater Quality

Cation	ppm as ion	ppm as CaCO ₃	Anion	ppm as ion	ppm as CaCO ₃
Calcium	650 - 845	1,625 - 2,113	Chloride	8,000-10,000	11,280 - 14,100
Magnesium	242 - 274	992 - 1,123	Sulfate	1100 - 1400	1,144 - 1,456
Sodium	5,600 - 6,200	12,208 - 13,516	Fluoride	118	310
pH	6.0-8.0				
m-Alkalinity	100-300				
Silica	200				

We also reached out to commercial and government contacts to make connections and obtain additional data.

We received power plant water quality data from a technology commercialization firm. While they would not reveal to us the name of the plant, they were able to share the cooling tower blowdown and FGD unit data. Unfortunately the data contained no information on key ions such as calcium, barium, iron, that we expect to be problematic—suggesting that the data is incomplete and not representative of most power plants. Finally, we were able to obtain both cooling tower and FGD water from Plant Bowen, a 3,200 megawatt coal-fired power plant located in Cartersville, Georgia. Plant Bowen has an EPRI Water Research Center for testing new water and carbon capture technologies and would be an ideal location to pilot COHO after completion of the system. Therefore, we chose the Plant Bowen CT and

FGD feeds as our targets for water studies.

- Coupon Testing on Simulated Feeds

To perform lab-scale testing, we created simulated feeds representing each type of wastewater, based on the data we received. Simulated feeds are required for consistent laboratory testing, since transport of feeds is logistically challenging and the feed typically changes over time and can lead to inconsistent results. The composition of simulated feeds were based on the Plant Bowen cooling tower (CT) and flue gas desulfurization (FGD) feed wastewater data we received. We simulated the feeds using ProDose software, by PWT Chemicals, a leading antiscalant manufacturer using their elemental ratios. When there was a range, we used the greatest value of the range. When both Total and Dissolved solutes were listed, we used Dissolved. Tables 2 and 3 show the composition of simulated CT and FGD feeds and the reagents respectively used to synthesize the feeds.

Table 2. Composition of Simulated CT Feed*

Ion	ppm	mM	Reagent	g/L
Calcium	94	2.35	CaCl ₂	0.260
Sodium	187.5	8.16	N/A	
Barium	0.64	0.0047	BaCl ₂ .2H ₂ O	0.00114
Iron	1.39	0.025	FeCl ₃ .6H ₂ O	0.00673
Carbonate	200.0	3.33	Na ₂ CO ₃	0.353
Chloride	169.3	4.77	N/A	
Sulfate	69.3	0.72	Na ₂ SO ₄	0.102
Fluoride	0.9	0.047	NaF	0.00199
TDS	726	726		
pH	9.1			

Table 3. Composition of Simulated FGD Feed*

Ion	ppm	mM	Reagent	g/L
Calcium	1962	48.95	CaCl ₂	5.433
Sodium	852.6	37.09	NaCl	7.545
Barium	0.21	0.0015	BaCl ₂ .2H ₂ O	0.00037
Iron	0.1	0.002	FeCl ₃ .6H ₂ O	0.00048
Carbonate	40.0	0.0007	Na ₂ CO ₃	0.071
Chloride	3471.5	97.92	NaCl	N/A
Sulfate	1692	17.61	Na ₂ SO ₄	2.502
Fluoride	10	0.526	NaF	0.02210
TDS	15573			
pH	7			

* N/A – No reagent added for that ion as it is already present from the addition of other ion.

Forward Osmosis Experiments

For the FO experiments, PFO membrane, manufactured by Porifera, was used. Membrane coupons of area 12.5 cm² were cut from the membrane roll and soaked in deionized water (DI) for 20 minutes prior to each experiment. The wet coupons were first tested under standard conditions (DI water vs 1 M NaCl at 25 °C) in the cross flow cell for membrane integrity and performance. For standard testing conditions, the active layer (skin) of the membrane was oriented towards the DI water (feed) and the support layer was faced towards the 1.0 M NaCl (Draw) solution. The feed and draw solutions were maintained at a constant temperature of 20 °C and a flow rate 3.72 cc/s. The tests were carried out for 10 minutes where the mass change was monitored on both feed and draw solution with balances every 20 seconds. The water flux was calculated from the mass transfer that occurred during this 10 minute period. The reverse salt flux (RSF) was calculated from the initial and final conductivity of the feed solution.

To generate the draw solution, deionized water (206.1 g) and dimethylcyclohexylamine (N(Me)₂Cy) (180.1 g, 1.42 mol) were placed in a bottle equipped with a gas diffuser and exposed to a steady stream of carbon dioxide for 3

hours while being stirred. The resulting solution was clear and homogenous (443.8 g) with a viscosity of 20.5 cP at 21.3 °C, pH of 8.8 at 22 °C, and density of 1.08 g/mL at 21 °C.

For water recovery studies from simulated CT and FGD feeds, the experimental conditions were similar to the standard test conditions. For examples with targeted water recoveries, the experiments were continued until the calculated feed mass was achieved. Either NaCl or N(Me)₂Cy was used as the draw solution for these experiments.

First, we performed flux experiments for both the CT and FGD feeds at different SPS concentrations. We initially measured the flux with 60 wt% SPS (the maximum concentration), then with diluted solutions. The flux measurements for CT feed and FGD feed are tabulated in Tables 4 and 5.

Table 4. FO membrane flux with CT Feed with SPS draw solution.

Feed	Draw	Flux (LMH)
CT Feed 13.45 mS/cm	60 wt% SPS, 12.58mS/cm	15.1
	30 wt% SPS, 27.9 mS/cm	15.4
	15 wt% SPS, 24.10 mS/cm	11.9

Table 5. FO membrane flux with FGD Feed with SPS draw solution.

Feed	Draw	Flux (LMH)
FGD Feed 21.44 mS/cm	60 wt% SPS, 12.58 mS/cm	12.6
	30 wt% SPS, 27.9 mS/cm	13.0
	15 wt% SPS, 24.10 mS/cm	7.9

These results show that for 60% and 30% SPS the FO flux is the same for both feeds. This is due to concentration polarization of the relatively high molecular weight dimethylcyclohexylamine. The lower concentration, 15 wt%, does show a flux reduction as expected. This means that for high osmotic feeds, increasing the SPS concentration may not increase flux. Therefore, the system may operate more efficiently (water concentrated for energy required to remove SPS) at SPS concentrations from 15 wt% to 30 wt%.

Water recovery experiments with simulated feed water were conducted using 15% SPS draw to determine the Maximum Achievable Recovery for the feeds. For these experiments, membrane performance was measured with standard tests before and after feed concentration to validate the integrity of the membrane and to measure the effect of scalants, if any, on the membrane.

We first concentrated the CT feed to a high water recovery rate, 80%, and found that there was no significant drop in flux. However, membrane testing and visual

inspection revealed the presence of scalants that fouled, but did not damage the membrane.

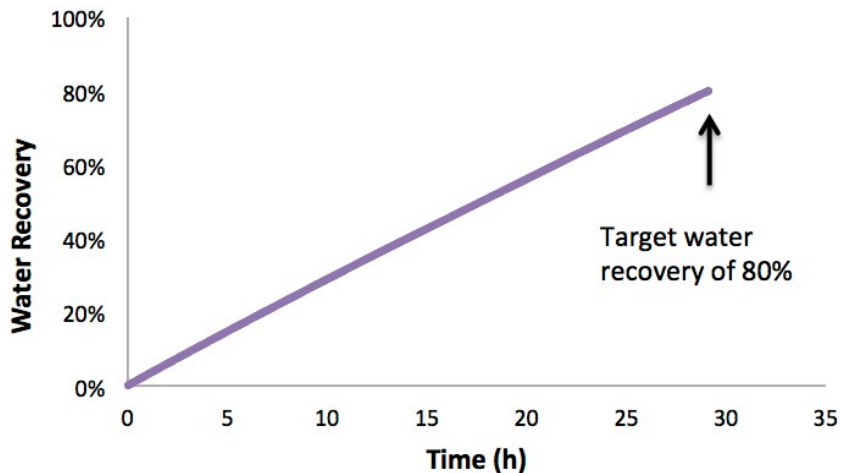


Figure 2. Concentration of 700 g of CT feed. The flux did not change (± 1 LMH) and the average flux remained high, 22 LMH (Figure 3).

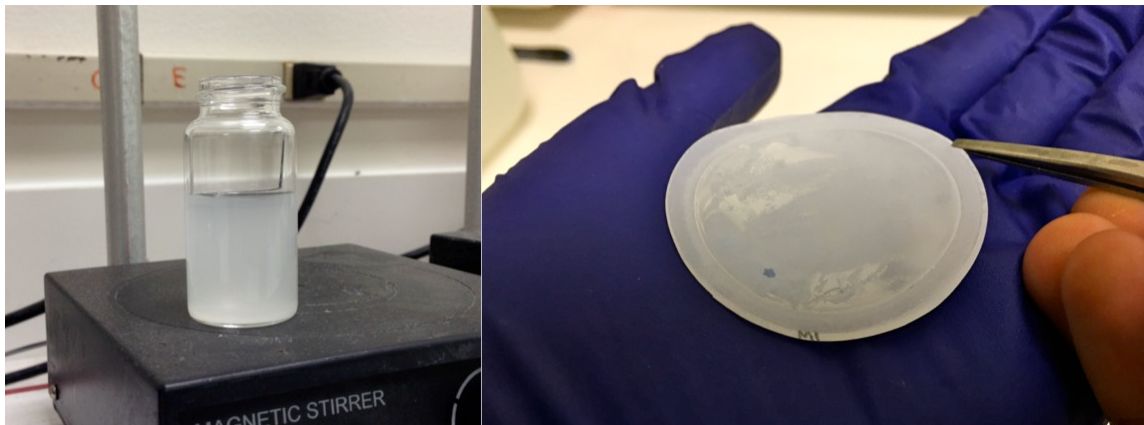


Figure 3. Left: Concentrated CT feed (80% water recovery rate). Right: Porifera membrane with CT scalants fouling the surface.

We reduced the target recovery rate for the CT feed to 60%, and repeated the concentration study with 15% SPS as the draw solution. We found the flux drop over time to be consistent, with some increase in RSF, suggesting that scaling and fouling was still forming. Therefore, the maximum achievable recovery for the CT feed, without pretreatment, is 50% or less.

We then studied the concentration of the FGD feed wastewater and found that the flux dropped rapidly above 50% water recovery.

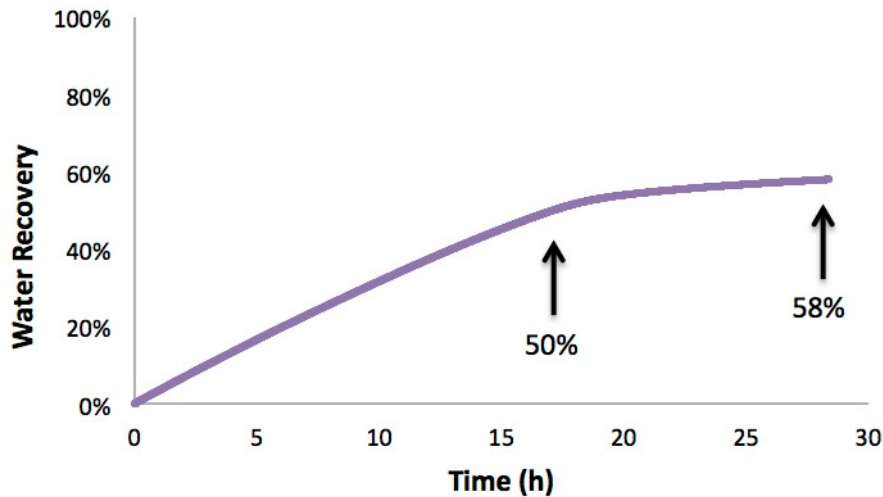


Figure 4. FGD Concentration approaching 60% water recovery.

Standard tests after the FGD concentration experiment showed that the membrane flux did not change much but the RSF increased significantly. This suggests that the membrane did not foul but damage to the skin occurred, probably from abrasion. Large crystals were visible in the FO concentrate.

No visible scaling or fouling of the membrane occurred.

The results suggest that the Maximum Achievable Water Recovery without pretreatment is 50% for the FGD feed, limited by damage to the membrane from scalants.

Both the CT Feed and the FGD Feed were limited by fouling or scaling of the



Figure 5. Precipitants clearly visible in FGD Concentrate.

membrane at 50% or less. We then studied methods for improving the maximum achievable recovery rate (see next section).

– Develop Methods to Increase Maximum Achievable Water Recovery.

Saturation Calculations

In the CT feed the main scalants of concern are BaSO_4 , CaF_2 and Fe. These scalants are of concern because, based on our calculations (see Table 6 below) they become supersaturated at high water recovery, potentially causing scaling, which would foul and compromise the membrane. In the FGD feed CaSO_4 , gypsum, also plays a major role.

Table 6. Saturations of scaling components of CT feed at 80% recovery.

Saturation Index SI %	Raw Feed	FO Conc	% Max SI with PWT
LSI	1.994	3.74	1.25
CaSO_4	2%	14%	3%
BaSO_4	1200%	8513%	85%
SrSO_4	0%	0%	0%
CaF_2	6%	332%	3%
SiO_2	0%	0%	0%
Iron	1390%	6583%	110%

Table 7. Saturations of scaling components of FGD feed at 70% recovery.

Saturation Index SI %	Raw Feed	FO Conc	% Max SI with PWT
LSI	-0.394	0.712	23.73%
CaSO_4	112.90%	494.80%	109.95%
BaSO_4	933.60%	3334.40%	33.34%
SrSO_4	0.00%	0.00%	0.00%
CaF_2	4238.90%	122846.4%	1023.72%
SiO_2	0.00%	0.00%	0.00%
Iron	100.00%	331.80%	5.53%

In the modeling studies, we found the most effect method of increasing the

water recovery of the feeds was to use a commercially available antiscalant (Spectraguard from PWT Chemicals). When the recommended antiscalant was used, the model showed that we should be able to reach high recovery without supersaturating the scalants. We studied the effectiveness of the antiscalant to reduce scaling for both the SPS draw solution as well as a traditional sodium chloride draw solution because of possible SPS and antiscalant interactions.

CT and FGD Coupon Studies with SPS Draw

For dewatering the CT feed, the lab coupon FO experiments with and without antiscalant were conducted to concentrate the feed wastewater to the given target recovery. After initial evaluation of the membrane performance, 400 ml of CT feed was dewatered using 4 L of 15 wt% SPS draw. Large draw volume was used to avoid osmotic dilution, as the feed was concentrated. The feed was concentrated overnight, for approximately 25 hours. Over the course of experiment, the average flux was around 8.3 LMH. It was observed that the flux increased by approximately 6% and the RSF increased by 30% after 60% water recovery of the CT feed, indicating the membrane was scaled and damaged during the concentration process. We then repeated the above experiment of CT feed concentration in the presence of antiscalant, where 400 ml of CT feed with antiscalant was dewatered using 4 L of 15 wt% SPS draw. We used the type and dosage of the antiscalant recommended by the Prodose program and added 6.45 ppm of Spectraguard 250 into the CT feed. Figure 1c and 1d show the water recovery from the simulated CT feed and the average flux during the course of the experiment when antiscalant was used. Although the average flux and hence the total time taken for at 60% water recovery remained the same, the membrane was intact, with no observable scaling or damage when antiscalant was used (Table 8).

Table 8. Membrane performance before and after water recovery from CT feed

	Flux (LMH)	RSF (g/L)	Comments
Initial	28.9	0.77	Without antiscalant
After dewatering CT feed	30.7	1.0	
Initial	32.3	0.812	With antiscalant
After dewatering CT feed	29.9	0.808	

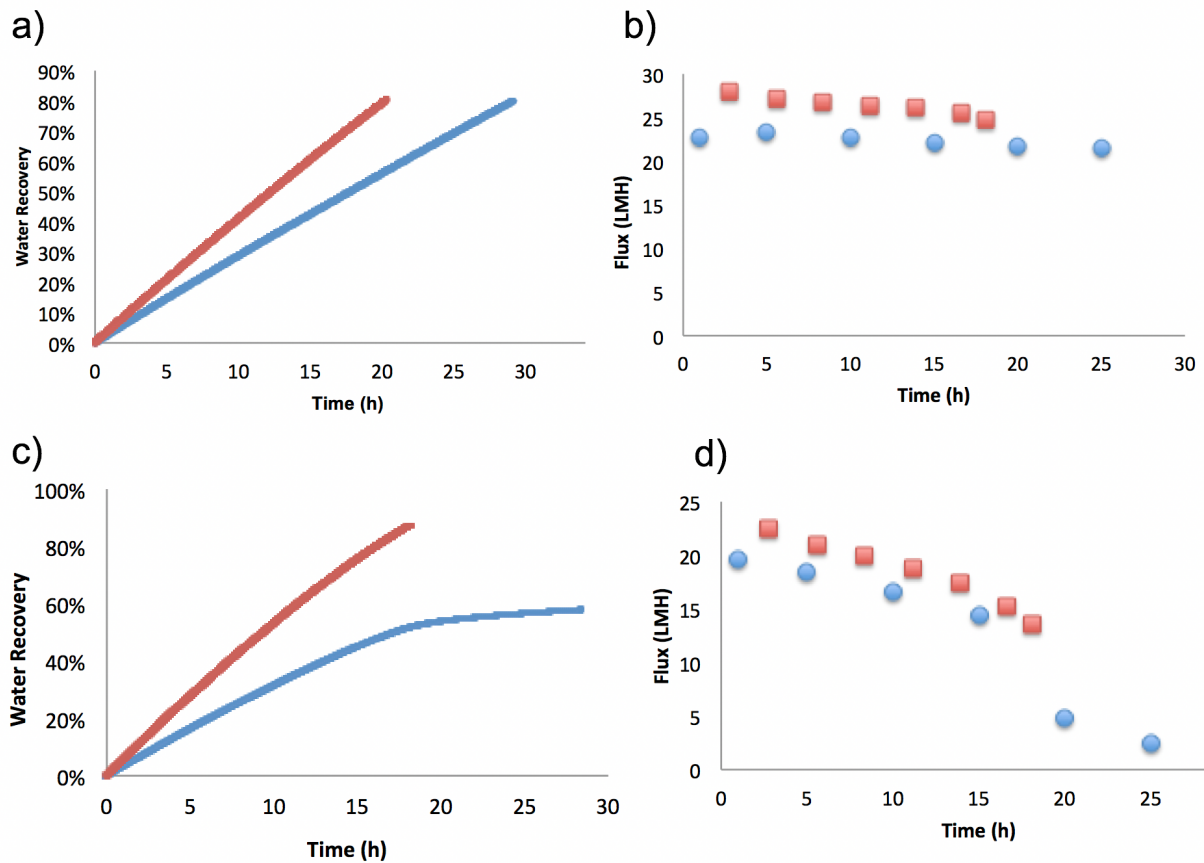


Figure 6: a) & b) Water recovery and flux from the simulated CT feeds without (blue) and with (red) antiscalant with 15 wt% SPS draw; c) and d) water recovery and flux from the simulated FGD feeds without (blue) and with (red) antiscalant with 15 wt % SPS draw.

A similar experimental procedure was followed for the simulated FGD feed where 400 mL of the feed was dewatered using 4L of 15 wt% SPS draw. The experiment was carried out with and without antiscalant as shown in Figure 6c and Figure 6d. Compared to CT feed, FGD wastewater feed has a higher TDS and is therefore more challenging to dewater. The major scalants in the FGD feed were sulphates (CaSO_4 and BaSO_4) and fluoride (CaF_2). These were already super saturated in the raw FGD feed (i.e., prior to dewatering). Even with use of antiscalant, which reduces the scaling potential of CaSO_4 and CaF_2 , the targeted water recovery was difficult to achieve .

To try to prevent scaling, we preconditioned the FGD feed using soda ash/lime conditioning and pH adjustment such that after 60% water recovery with antiscalant, the concentration of calcium super saturation limits of the scalants would not be attained. The initial experimental data with pretreated FGD feed was promising. Although we saw a small increase in RSF, we were able to optimize the pretreatment process to achieve our desired target recovery without compromising membrane performance. Table 9 details the results of these experiments. The data shows that for concentration of the FGD feed preconditioning is a critical step. Without it, the membrane would become severely damaged through scaling.

Table 9. FO membrane performance before and after FGD concentration with 15 wt% SPS.

	Flux (LMH)	RSF (g/L)	Comments
Initial	24.3	0.655	Without antiscalant
After dewatering FGD	25.0	2.244	
Initial	24.1	0.46	With antiscalant
After dewatering FGD	30.4	2.12	
Initial	28.6	0.89	With pretreatment and antiscalant.
After dewatering FGD	29.7	1.1	

CT and FGD Studies with NaCl draw

We also carried out water recoveries of the simulated wastewater feeds with a standard NaCl draw to see if this impacted scaling behavior. Initial membrane performance was evaluated under standard testing conditions to verify membrane integrity. The water recovery experiments were then conducted, both with and without use of antiscalants.

For the CT feed, we used 6.45 ppm of PWT Spectraguard 250. The CT feed (700 g) was dewatered using 1 M NaCl draw (7 L) for both the experiments. Figures 2a and 2b show the water recovery from CT feed without (blue) and with (red) antiscalant. With antiscalant, it took less time (20 hours) to reach target recovery of 80%, because of an overall higher average flux of 28 LMH. Without antiscalant, it took 28.8 hours to reach the target recovery with an average flux of 22.4 LMH. After dewatering the CT feed, both sides of the membrane were flushed for a minimum of 1 hour until salt no longer desorbed from the membrane. Then the membrane performance was measured again using standard conditions. Table 10 shows the membrane performance before and after dewatering CT feed. Without antiscalant there was 10% drop in flux when we concentrated to 80% recovery, whereas with antiscalant the flux stayed the same. With the NaCl draw solution, we achieved a recovery target of 80% with the antiscalant without any reduction in flux or fouling. Therefore, the maximum achievable water recovery will likely exceed 90% recovery for CT feed dewatering with NaCl draw solution.

Table 10. Membrane Performance for CT Feed Measurements

	Flux (LMH)	RSF (g/L)	Comments
Initial	27.8	0.34	Without antiscalant
After dewatering CT feed	25.0	0.29	
Initial	28.2	0.35	With antiscalant
After dewatering CT feed	28.7	0.36	

We then performed an identical test with the FGD feed. We used 500 mL of feed and 5 L of 2M NaCl as the draw solution. We used a higher draw concentration because the feed has a much higher TDS. The dewatering experiments were conducted both with and without antiscalant. Our goal was to identify the maximum achievable recovery without any discernable change in flux.

Without antiscalant, we found that the FGD feed dewatered consistently for about 17 hours (50% recovery) whereupon a noticeable reduction in flux occurred. The experimental results showed a clear drop in flux after the solution passed 50% recovery, from nearly 20 LMH down to less than 5 LMH. Even after 25 hours the water recovery was around 60%.

Table 11. Membrane standard tests before and after FGD Concentration in the presence of antiscalant to 87% recovery.

	Flux (LMH)	RSF (g/L)
Initial	22.5	0.38
After FGD	19.9	0.53

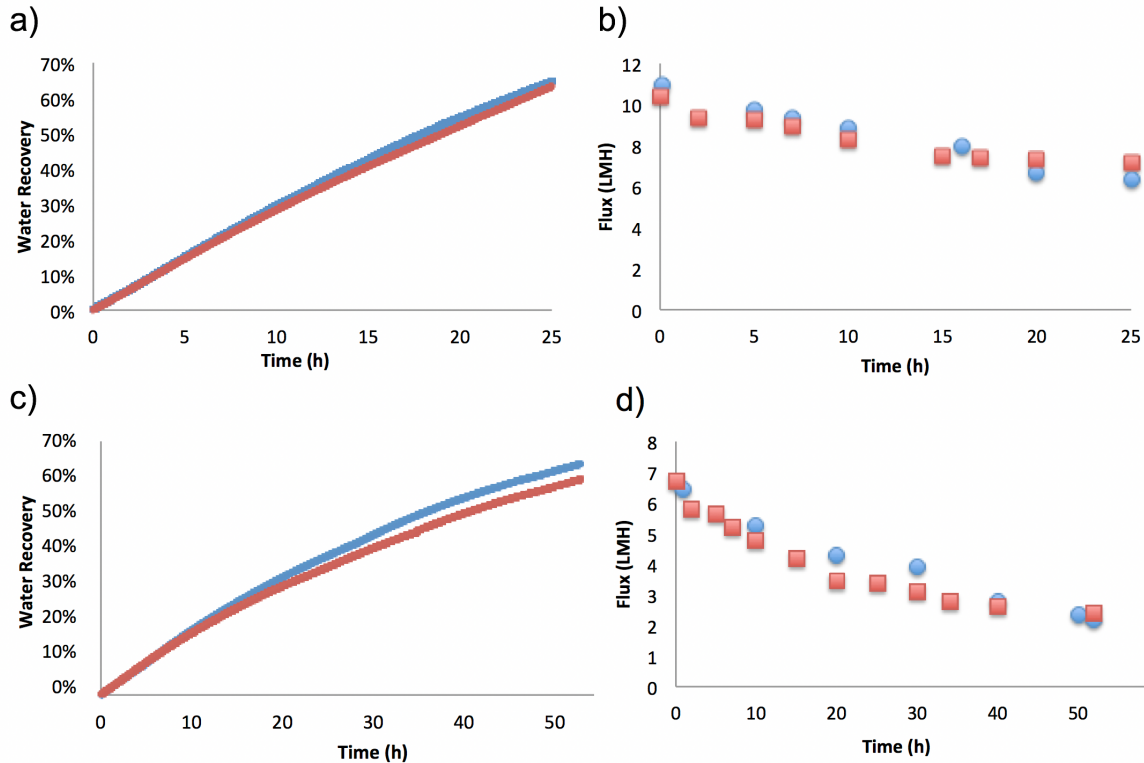


Figure 7: a) & b) Water recovery and flux from the simulated CT feed without (blue) and with (red) antiscalant with NaCl draw; c) and d) water recovery and flux from the simulated FGD feeds without (blue) and with (red) NaCl draw For CT feed, standard 1M NaCl was used as draw. Owing to higher TDS of FGD feed, 2M NaCl was used as the draw.

With antiscalant, we were able to dewater 87% of FGD feed with over an 18 hour time period, as shown in Figure 7. We found that the flux dropped gradually over time as the feed became more concentrated. Standard tests after the FGD concentration with antiscalant showed that the membrane flux dropped by 11% and that the RSF increased by slightly (see Table above). This suggests that there may be minor damage to the skin of the membrane, probably from abrasion. Therefore, we reduced the target recovery for the FGD feed to below where membrane damage may occur, 75%.

Investigation of Asymmetric Membranes

While Porifera's PFO membrane, a thin-film composite membrane, has excellent flux and selectivity, a disadvantage of the membrane structure is that the 100-nm thick skin layer is easily damaged by scalants, such as calcite and gypsum. Both of these scalants are present in the CT and FGD feeds. In addition, the thin skin layer is sensitive to the presence of chlorine in the feed; chlorine-based cleansers to remove biofouling cannot be used. Therefore, we also investigated the performance of a unique asymmetric membrane. Asymmetric membranes have a thicker skin layer, and may be more tolerant to the types of scalants present in power plant wastewaters and the chlorine based cleansers that they use with them.

We prepared an asymmetric membrane using a proprietary polymeric material that is known to be compatible with the SPS draws we are studying for this work. Preparation was performed via phase inversion—whereby a polymer is dissolved in a solvent and then cast on a substrate, such as a glass plate, to form a thin film. Often, a nonwoven or woven support, such as a fabric or a mesh, may be used to lend additional mechanical strength to the produced membrane. The film, support, and plate are then immersed in a non-solvent, typically water, and the solvent diffuses out of the membrane into the nonsolvent, resulting in a porous polymeric film on the support. Usually the phase inversion produces a membrane with large micropores at the bottom and a dense skin layers on top. The membrane flux and rejection can be “tuned” by controlling the thickness of the membrane (ideally the dense layers are less than 2 microns) and by controlling pore size and the density/openness of the support layers.

We tuned the membrane pore size and density by altering the salt and polymer concentrations of the solutions used to cast the membrane on a support.

Volatile solvents were added to the polymer solution to control the uniformity of the dense skin layers and its thickness. The rate of solvent evaporation was optimized by heating the membrane cast on a support and the nonsolvent bath temperature and conditions.

A 15 wt% polymer solution was prepared by mixing polymer to a solvent mixture under inert atmosphere, maintained at approximately 95 deg. C. The polymer solution was diluted to approximately 12 wt% by the addition of volatile solvent, such as proprietary Solvent A or Solvent B. A thin film of suitable thickness (approximately 60 microns) was cast directly on a glass plate or on a woven support on a glass plate. The cast membrane was heated at high temperature and then placed into a nonsolvent aqueous bath for a few minutes.

Table 12. Initial Nomex Asymmetric Membrane Results (Feed: DI Water, Draw: 1 M NaCl).

Polymer	Additive Solvent	Support	Flux (LMH)	RSF (g/L)
Proprietary	Solvent A	none	8	1.2
Proprietary	Solvent B	none	10	0.8
Proprietary	Solvent A	yes	4	2
Proprietary	Solvent B	yes	6	1.8

Results are displayed in the table above. The variation of flux indicates that that there is a significant difference between the membranes produced without a support and the membranes with support. The flux may vary due to differences in morphology.

We tested the asymmetric membranes against the simulated FGD feed, and found that scaling still induced damage, despite being a thicker membrane. Therefore, we focused our efforts on the addition of anti-scalants and feed preconditioning as discussed in the prior section.

- CO₂ Capture Optimization

To simulate the capture of carbon dioxide from post-combustion flue gas, we studied the CO₂ scrubbing ability of the draw. We chose to use Dimethylcyclohexylamine (DMCHA) since it is the most readily available SPS draw. We found that bubbling a CO₂:N₂ mix through a heterogeneous mixture of DMCHA and water produces an ammonium bicarbonate solution suitable for use as an osmotic draw. Bubbling a 15:85 CO₂:N₂ volume mix for 17 hours produces a 4.86 molal solution by amine concentration or a 47.4 wt% solution with a projected osmotic pressure of 215 atm. Bubbling a 6:96 CO₂:N₂ volume mix for 20 hours produces a 4.17 molal solution by amine concentration or a 43.6 wt% solution with a projected osmotic pressure of 184 atm. These may not be maximum achievable concentration levels, but they do demonstrate that any flue gas bubble-mixed with dimethylcyclohexylamine will generate a draw solution.

Table 13. Draw Generation using post-combustion flue gas.

SPS Draw	Conc. using pure CO₂	Conc. using 15:85 CO₂:N₂	Maximum wt% using 6:96 CO₂:N₂
DMCHA	77 wt%	47 wt%	44 wt%

Operate and Model the System.

– Operate and Optimize COHO system.

Lab-scale testing of COHO was specifically designed to mimic field operations. The draw solution was generated using the synthetic post-combustion flue gas, as discussed in the previous section titled CO₂ Capture Optimization. Synthetic CT or FGD feed was concentrated, diluting the draw solution. The draw solution was regenerated by heating the solution and then flowing through a nozzle to induce phase separation. We found that we were able to remove 75% of the draw solute

from its initial maximum concentration at low-grade heat temperature (70 °C). We increased the temperature in order to achieve higher recovery. At 95 °C, the draw removal was 94%. Changing the concentration of the draw did not change the removal efficiency.

Figure 8 shows the clearly visible separation between the organic amine (top layer) and aqueous portion of the solution (lower) achieved during phase separation. The conductivity of the aqueous was measured to be 7.1 mS/cm, equivalent to 2.5 wt % of the SPS amine (residual) in water. The residual SPS amine was separated from the solution using RO.

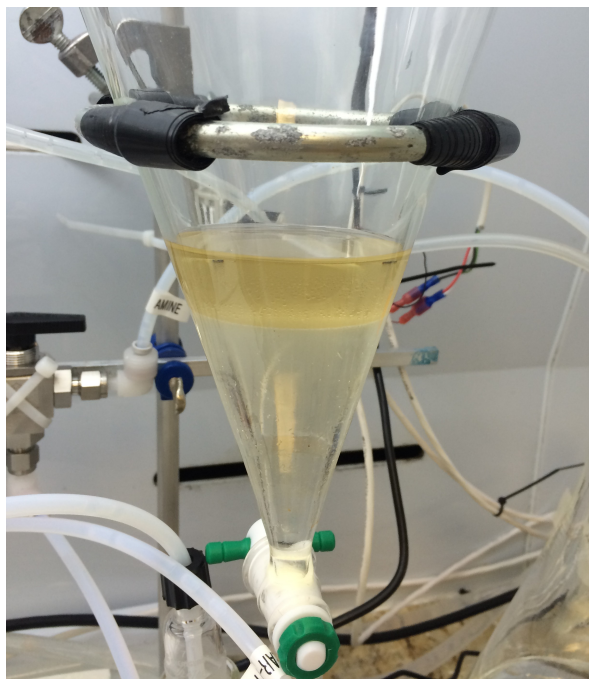


Figure 8: Photo showing the separation of organic amine (top layer) from the aqueous portion (bottom layer) of the solution at 95 C.

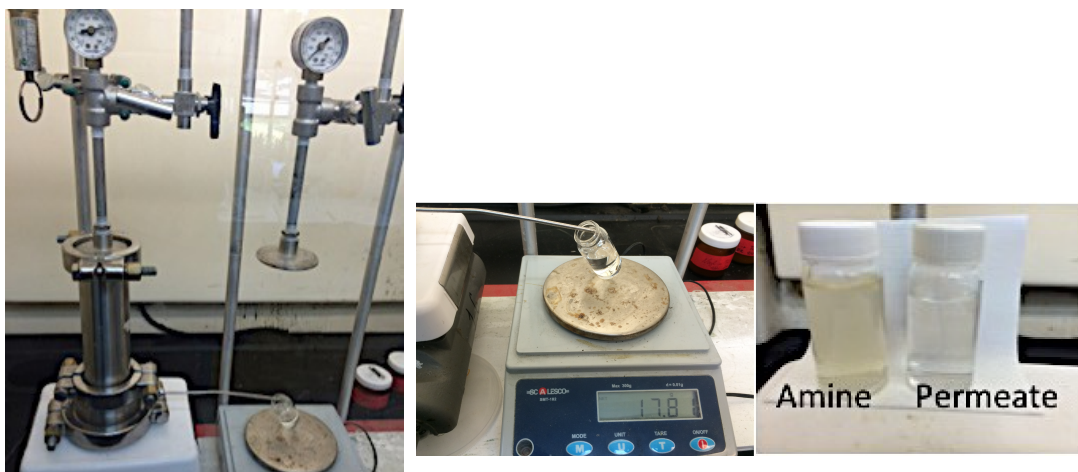


Figure 9: Left: Photo of the RO setup at Porifera used to remove the trace amount of amine from the aqueous portion of the solution. Middle: Permeate collection during the RO process. Right: The end products after RO process.

Table 16 summarizes the weight and conductivity of solution before and after the RO process. The permeate recovered was 50.06 wt% of the total initial solution with a conductivity of 0.125 mS/cm. The mass of the concentrated amine solution (reject) recovered was approximately 32 g (a few milliliters were lost while transferring the amine solution out from the cell) with the conductivity of 13.06 mS/cm giving an overall rejection of the amine of 99.1%. The initial flux during the RO process was quite high, 21.6 LMH.

Table 14. Trace SPS separation from the aqueous portion of the solution.

SPS concentration in the aqueous portion	Initial weight (g) of aqueous portion of the solution.	After RO permeate recovered (weight and conductivity)	After RO amine recovered (weight and conductivity)
2.5 wt% 7.1 mS/cm	74	37.05 g and 0.125 mS/cm	32.21 g and 13.06 mS/cm

SPS regeneration

For SPS regeneration after water recovery, the diluted SPS draw was heated to different temperatures in the jacked flask. This allowed us to understand the switching

behavior of the SPS draw. The heated draw was circulated in a closed loop by pumping the solution out and spraying it back into the jacked flask over different time periods. We then transferred the draw into a separation funnel and allowed it to cool to room temperature. A clearly visible separation between the organic amine and aqueous portion of the solution was achieved during phase separation. We then passed the aqueous portion of the solution through an RO filter for trace removal of any amine that may not have separated.

Trace Removal of Draw Solute via RO

Trace removal of remaining amines was performed with a Hydranautics SW-C5 RO membrane. A “dead-end” RO cell was used where the solution was pressed against the membrane using compressed nitrogen gas. The aqueous portion was collected in a separate beaker and an initial weight and conductivity measurements were recorded. The weighed aqueous solution was then transferred into the RO cell and pressurized to 800 psig by using N₂. To mitigate the effect of external concentration polarization (CP), the solution was aggressively stirred using a magnetic stirrer. The removal of water (permeate) from the aqueous solution during the process was monitored and collected.

Operation Summary –

The COHO system was operated according to the Test Plan shown below with results from the preceding sections summarized.

Table 15. COHO Test Plan and Result Summary

Step	Description	Anticipated Result	Actual Result
1	Operate FO componentry using pure water feed for 15, 30, and 60 wt% SPS. A feed will be concentrated and a draw solution will be diluted using a target recovery of 50 – 70% at room temperature while monitoring mass transfer over time.	Measure water flux dependence on concentration on the system.	Flux for 15, 30, and 60 wt% SPS was measured. Although the higher concentrations achieved higher osmotic pressures, flux was limited by concentration polarization.
2	Operate SPS separation componentry for 15, 30, and 60 wt% SPS. The diluted draw will be heated and passed through a nozzle into a separation funnel to separate the organic amine from the aqueous portion of the draw solution.	Measure temperature dependence of removal. Determine minimum operational temperature for each concentration.	Achieved. We found that higher temperatures were required for high SPS removal (>70 deg. C). This was unexpected. Gen 2 SPS is recommended for future work (not studied as part of this work).
4	Operate RO polish componentry. The aqueous portion (Step 2) of the draw solution will be passed into a RO unit and pressurized (~ 800 psi), producing a clean water permeate and concentrated aqueous portion.	Measure efficiency of SPS removal of RO to determine if additional polishing steps will be required in a commercial system.	Achieved. The RO unit was able to effectively polish the aqueous portion of the draw solution with >99% rejection.
5	Operate SPS regeneration conditions with pure CO ₂ and with dilute CO ₂ for 15, 30, and 60 wt% SPS. The concentrated aqueous portion (Step 4) will be returned to the draw tank, recombined with amine, and passed through a CO ₂ gas contactor to regenerate the draw solution used in Step 1.	Measure regeneration time and efficiency for carbon capture capabilities.	Achieved for 15 wt% SPS. The higher concentrations were not required for the feed concentrations that were anticipated for the system.
6	Operate system with synthetic feeds and gas feeds. Replace pure water and gas streams with synthetic streams to model processing at a power plant.	Identify the ideal SPS concentration and operation conditions of COHO system for synthetic feeds. Supply data for economic analysis.	Achieved. Addition of antiscalant is recommended for both feeds with preconditioning (pH adjustment) of the FGD feed.
7	Optimize COHO: Modify system or process to improve efficiency. Here we may modify the system slightly, and use anti-scalants or additives to aid in SPS separation and regeneration.	Remeasure processing of synthetic feed. Supply data for economic analysis.	Antiscalants were used for both simulated feeds, in addition to pH adjustment for the FGD feed.

– Develop techno-economic model of COHO system.

Using the data collected in the previous section, we built a cost model and performed a techno-economic analysis to compare the capital and operating cost of COHO against competing technologies. The target recoveries were fixed at 90% for both streams with a feed flow of 480 m³/day.

Draw Recovery Estimate

We began by estimating the capital costs of the draw recovery portion of the system based on Idaho National Laboratory's preliminary engineering design basis for the FO SPS system [10]. The total fixed capital costs include direct capital costs and indirect capital costs. Direct capital costs include inside battery limits (ISBL) and outside battery limits (OSBL) cost contributions. ISBL costs include equipment and associated components that act upon the primary feed stream of the process, while OSBL costs include utilities, common facilities, and other equipment not included in the ISBL definition and may include systems that support several process units. The ISBL capital costs include the equipment costs for the major process components, which are summarized in the table below. The SPS FO process does not require inventory of raw materials, products or by-products; working capital costs will therefore only include SPS, CO₂, and spare parts inventory requirements. In the current analysis, working capital costs are estimated as 5% of the ISBL + OSBL costs.

Table 16. Estimated equipment costs for draw recovery on a 20 m³/hr SPS FO process

Component	Sizing	Value	Equipment	Total Installed	Source
degasser					
preheater	heat transfer area	318 m ²	\$52,900	\$182,100	a
vessel	volume	31 m ³	\$101,700	\$402,700	a
heat exchanger	heat transfer area	10 m ²	\$10,200	\$70,500	a
spray nozzles	flow rate	467 m ³ /hr	\$21,400	\$49,200	b
circ pump	flow rate	467 m ³ /hr	\$39,200	\$90,300	b
decanter (3 stages)					
vessel	volume	9.0 m ³	\$39,300	\$90,400	b
circ pump	flow rate	47 m ³ /hr	\$5,400	\$12,500	b
gas contactor					
membrane	membrane area	1,206 m ²	\$24,100	\$55,500	c
pump	flow rate	4.8 m ³ /hr	\$900	\$2,100	b
heat exchanger	heat transfer area	33 m ²	\$18,300	\$87,300	a
NF polishing filter	membrane area	383 m ²	\$7,700	\$17,600	c
RO polishing filter	membrane area	833 m ²	\$16,700	\$38,300	c
pumps					
SPS circulation	flow rate	24 m ³ /hr	\$900	\$2,100	b
NF/RO feed	flow rate	23 m ³ /hr	\$8,300	\$40,500	a
HTF pump	flow rate	50 m ³ /hr	\$1,800	\$4,200	b
gas compressor	flow rate	900 m ³ /hr	\$193,300	\$263,700	a
compr exh cooler	heat transfer area	23 m ²	\$15,900	\$84,600	a

Sources: (a) Aspen Process Economic Analyzer (b) vendor pricing listed or quoted as of June 2016 (c) assumed membrane cost of \$20/m² for gas diffusion, NF, and low- pressure RO membranes (Pabby, Rizvi, and Sastre 2015);

For process components where the equipment costs were obtained from vendor pricing/quotes or assumed costs, an installation factor of 2.3 was used to estimate the total installed cost. This factor was obtained by summing the installation factors for the installation categories identified in Table 17. The installation factors are lower than those recommended for a fluid-based chemical process by Sinnott and Towler (2009) due to the relatively small scale process

considered and the assumption that the process will be installed as a modular unit, which will result in decreased installation costs. The installation factors suggested by Sinnott and Towler for a fluid-based chemical process are included in Table 17 for reference.

Table 17. Factors for estimation of fluid-based process fixed capital costs

Category	Value used in current study (modular process assumed)	Value suggested by Sinnott and Towler (2009)
Equipment erection	0.1	0.3
Piping	0.5	0.8
Instrumentation and control	0.3	0.3
Electrical	0.2	0.2
Civil	0.1	0.3
Structures and buildings	0.1	0.2
Lagging and paint	0.0	0.1
Installation Factor	2.3	3.2

The OSBL costs are calculated as a percentage of the ISBL costs. Sinnott and Towler (2009) recommend the OSBL costs be estimated as 30% of the ISBL costs. However, many of the OSBL items identified by Sinnott and Towler are either accounted for as ISBL costs, or are expected to be available to the SPS FO process installation due to the installation of the process at an oil & gas production site. Therefore, the OSBL costs for the current analysis are evaluated as 20% of the ISBL capital costs. Table 18 provides a listing of the OSBL costs that are intended to be included in the 20% estimate in the current analysis, as well as a summary of the OSBL costs that are not required or should already be in place for the wastewater treatment application.

Table 18. OSBL costs included and excluded from economic evaluation. Adapted from Sinnott and Towler (2009).

Item	Description	Notes
OSBL capital costs required for SPS FO process installation		
Water	water demineralization, waste water treatment, site drainage and sewers	
Piping	pipe bridges, feed and product pipelines	
Transport	tanker farms, loading facilities	
Analytical	laboratories, analytical equipment, offices, central control room	
Utility: Cooling	cooling towers, circulation pumps, cooling water mains, cooling water treatment	
OSBL capital costs NOT required for SPS FO process installation		
Utility: Electric	electric main substations, transformers, switchgear, power lines, etc.	assumption of use of existing infrastructure at production site and purchase of electrical power
Utility: Power	power generation plants, turbine engines, standby generators	assumption of use of existing infrastructure at production site and purchase of electrical power
Utility: Steam	boilers, steam mains, condensate lines, BFW treatment plant, supply pumps	thermal energy to be provided by feed stream
Utility: Air	air separation plants	N/A
Maintenance	workshops and maintenance facilities	existing production site infrastructure
Emergency Services	emergency services, fire-fighting equipment, fire hydrants, medical facilities, etc.	existing production site infrastructure
Security	site security, fencing, gatehouses, landscaping	existing production site infrastructure

Indirect capital costs include design and engineering and contingency costs. It is assumed that a standard design for the SPS FO process for industrial wastewater treatment (including blowdown water) will be developed for deployment at multiple sites. The use of a standard, or module-based, design will reduce the design & engineering costs for installation number N (with $N \gg 1$) in such a deployment scenario. It is likely that the majority of engineering costs may be associated with feed water pretreatment, which will be an application-specific cost depending on the feed water composition and existing wastewater site infrastructure. Design & engineering costs in

the current analysis are estimated as 10% of ISBL + OSBL costs, which is on the lower end of the range recommended by Sinnott and Towler (2009) for the reasons listed above. Contingency costs to cover changes in commodity pricing, currency fluctuations, and problems/issues associated with the overall project schedule are estimated as 10% of the ISBL + OSBL costs. Additionally, this technology is a Class 4 project according to AACE cost estimate classification system as additional piloting is required before full scale commercialization. Therefore, estimates have an expected accuracy range of -15% to +30%.

COHO System Analysis

The FO flux measured with the simulated feeds was used to estimate the capital costs of the FO system using Porifera's targeted membrane costs. The FO System CAPEX includes membrane elements and hardware, frames, instruments, controls, and piping connections that summed to \$340,000 for the CT feed and \$500,000 for the FGD feed. The FGD feed has a higher capital cost because the lower flux requires more membrane area. The FO CAPEX was combined with the Draw Recovery CAPEX that was detailed in the previous section. Our total system CAPEX sums to \$2,153,000 for the CT feed and \$2,513,000 for the FGD feed.

Table 19. COHO Cost Analysis

		CT Feed	FGD Feed	units
Total water	Water recovery	90%	90%	%
	Feed flow	480	480	m ³ /day
	Permeate Flow	432	432	m ³ /day
	Permeate Flow	157680	157680	m ³ /year
	Reject Flow	48	48	m ³ /day
Water Quality	Feed TDS equivalent	5,000	12,700	ppm TDS
	Reject TDS equiv	50,000	127,000	ppm TDS
Flux	FO Flux	8	5	lmh
Energy per unit of permeate	Unit Electricity Use	1.9	2	kWh/ m ³
Porifera CAPEX	FO system	\$340,000	\$500,000	
	Draw Recovery system	\$1,813,000	\$2,013,000	
	Total	\$2,153,000	\$2,513,000	
CAPEX Unit Cost \$/cmd capacity		\$4,485	\$5,235	
5 year \$/m³ without amortization		\$2.46	\$2.87	
Porifera OPEX est	FO system	\$32,000	\$65,000	
	Draw Recovery system	\$20,000	\$145,000	
	Total	\$52,000	\$210,000	
	\$/m3	\$0.02	\$0.07	
OPEX Unit cost		\$0.02	\$0.07	
Total 5 year unit cost without amortization		\$2.47	\$2.94	
Total 5 year unit cost with amortization		\$2.74	\$3.24	

The FO system OPEX includes membrane replacement and cleaning chemicals (cleaning and draw agent consumables), electricity for feed circulation (\$0.08/kWh). The Draw Recovery system OPEX includes electrical power, process heating, and a labor estimate [11]. The CT feed OPEX is estimated to be \$0.02/m³ and the FGD feed OPEX is estimated to be \$0.07/m³. The FGD Feed is higher because of the increased membrane from the lower flux rate, increased chemical use and heating and chilling loads.

We then used the 5-year amortized cost (3.5%) to compare COHO with competing technologies for FGD wastewater treatment. Power plant feeds are typically concentrated using several different types of thermal evaporators. We found costs on comparable multistage evaporators (MSE) [11], mechanical vapor recompression (MVR1) [11], a second mechanical vapor recompression system (MVR2) [12] and multieffect distillation (MED) [12]. In addition, we included the cost estimate of a recent player in the power plant wastewater market, Gradiant Corporation, that produces a modified thermal evaporator system [12]. For this savings estimate, we limited the case study to FGD wastewater treatment to develop a clear comparison case. However, COHO can treat both CT blowdown as well as FGD wastewater to further decrease the unit cost per m³.

Table 20. Comparison of COHO's cost with competing technologies to treat FGD wastewater.

	COHO	MSE	MVR1	MED	MVR2	Gradient
Water Recovery (%)	90	60	60	95	95	95
Feed Flow (m3/day)	480	397	397	528	480	480
Total CAPEX	\$2,513,000	\$2,800,000	\$4,000,000	\$1,413,043	\$869,565	\$579,710
OPEX Unit Cost	\$0.07	\$4.40	\$4.65	\$26.09	\$17.39	\$4.49
Total 5-year unit cost with amortization	\$3.24	\$8.68	\$10.76	\$27.71	\$18.49	\$5.23

In a direct comparison of the unit cost per m³ of feed water treated, COHO is significantly less than other competing technologies (Figure 10). While in some cases the COHO CAPEX is similar (MSE, MED), COHO has a much lower OPEX because of the reduced energy consumption. The MED has the highest cost because of the thermal loads and system complexity. The Gradient technology claims to have a hybrid membrane and system operation improvements to reduce costs.

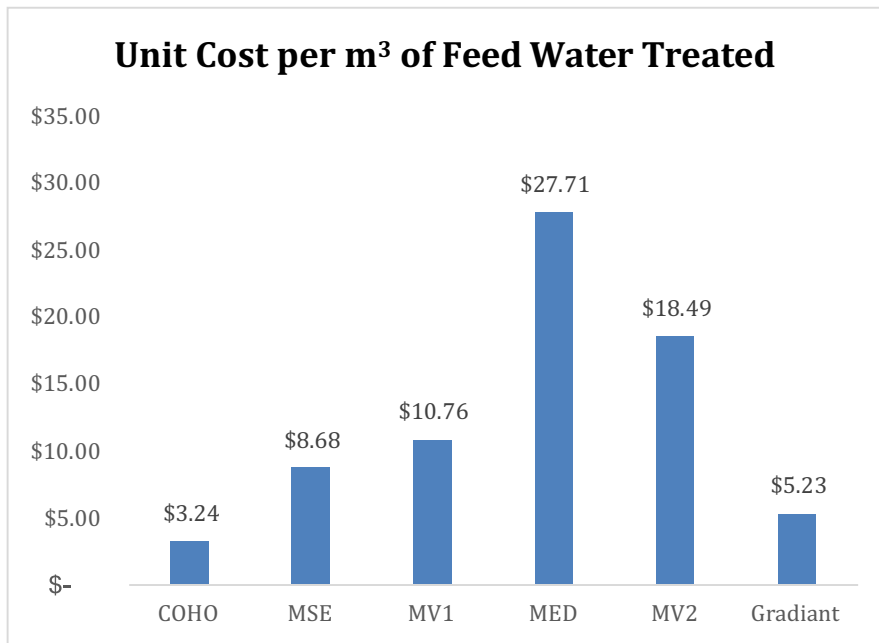


Figure 10. Unit Cost of FGD Feed Water Treated.

We also considered the competing technologies in unit cost per m³ of water reused, to account for the varying recovery rates (Figure 11). In that case MSE, MV1, and MV2 are similar to each other. The MED remains the most expensive technology, and the Gradient Energy showing savings over conventional technologies. However, COHO remained the least expensive option by a large margin.

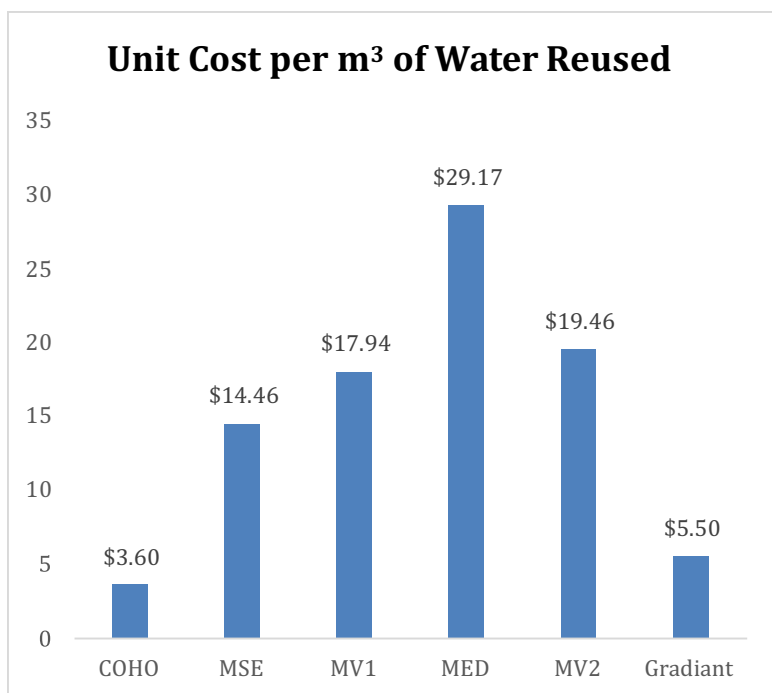


Figure 11. Unit Cost of FGD Feed Water Reused.

3. Conclusion

For this project, we demonstrated on the bench-scale (in liters) that COHO can efficiently dewater challenging simulated CT and FGD feeds using carbon dioxide from flue gas. This presents a great opportunity with benefits to the environment as well as savings to the customer. First, we developed simulated feed recipes using data from Plant Bowen. The feeds had moderate total dissolved solids, but significant amounts of scale forming compounds, including calcium, sulfate, and iron. We found that without antiscalant present, as a “raw” feed, both feeds induced damage in the membrane at 50% water recoveries. However, with the addition of commercial antiscalant, COHO was able to successfully concentrate the CT feed to 60% recovery and the FGD feed, with preconditioning, to 60% recovery with the SPS draw. With an NaCl draw, the recoveries were higher, 80% for the CT Feed and 75% for the FGD feed. We expect that the next generation SPS in development by INL will increase membrane retention, improving

antiscalant performance.

In addition to concentration of the feeds, we tested the process using the SPS draw solution to remove 99% of the carbon dioxide from simulated flue gas and found that the draw solution was successfully generated with even dilute CO₂ concentrations typically found in flue gas. This demonstrates that COHO can be used to remove carbon dioxide from flue gas, while reducing wastewater volumes and generating clean water. We tested the draw removal step, and found that while higher temperatures were required for removal than we desired (above 70 deg. C), we were able to produce clean permeate after following thermal regeneration with a reverse osmosis step with greater than 99% rejection.

Finally, we performed a techno-economic model of the COHO system by estimating the 5-year amortized CAPEX of the draw recovery system with the FO system, and combining it with the OPEX for both the CT Feed and the FGD Feed. In addition, we compared the costs to competing evaporating technologies used today. We found that while the CAPEX was similar in most cases, the OPEX savings was significant enough to result in significant savings on a unit cost per m³ basis. For example, compared to MSE, the cost of installing and operating COHO would be recovered within 3 years.

4. Recommended Next Steps

Generally, the best pathway to market for any water treatment technology is to first deploy small units in high margin markets that do not require long annuitizing periods. This allows the technology to benefit from real world optimization/learning and permits a wide array of industries with water treatment needs to evaluate the initial performance before adoption into the broader market. It would be ideal to deploy

COHO at the smallest continuous operation scale possible and demonstrate it in a market like the treatment of oil and gas water. This will allow the technology to be proven on a smaller scale prior to construction of a large-scale system used to address the high-volume needs of a coal fired power plant.

Given the success of this and other projects, COHO and SPS FO is at a point where it is ready to move from batch-mode systems to a continuous system. In related work, INL has had success on a project that uses SPS FO to treat high TDS produced water on the 25 gallon per day scale in batch mode. While batch-mode systems, with recirculation of the feed and draw streams, can process smaller volumes, the draw streams must be operated with a large osmotic over-pressure to ensure the diluted draw exceeds the final feed osmotic pressure. In Porifera's FO commercial systems, the feed is dewatered continuously and the draw stream is operated in counter current against the feed stream, so that the average osmotic over-pressure is consistent and much smaller on average compared to co-current. Counter current operation has the benefits of consistent flux during concentration and reduced draw solute concentration. However, for continuous operation in counter current mode the pilot scale is larger compared to batch processing. From the equipment requirements, we estimate the pilot should operate at approximately 1,500 gallons per day. Demonstration at this scale will allow the system to be automated, operated in continuous manner, and piloted in the field.

5. References

- [1] T. Y. Cath, A. E. Childress, M. Elimelech, Forward osmosis: Principles, applications, and recent developments, *Journal of Membrane Science* 281 (2006) 70–87.
- [2] S. Zhao, L. Zou, C. Y. Tang, D. Mulcahy, Recent developments in forward osmosis: Opportunities and challenges, *Journal of Membrane Science* 396 (2012) 1–21.

- [3] C. Klaysom, T. Y. Cath, T. Depuydt, I. F. Vankelecom, Forward and pressure retarded osmosis: potential solutions for global challenges in energy and water supply, *Chem. Soc. Rev.* 42 (2013) 6959–6989.
- [4] E. Cornelissen, D. Harmsen, K. Dekorte, C. Ruiken, J. Qin, H. Oo, L. Wessels, Membrane fouling and process performance of forward osmosis membranes on activated sludge, *Journal of Membrane Science* 319 (2008) 158–168.
- [5] A. Achilli, T. Y. Cath, A. E. Childress, Selection of inorganic-based draw solutions for forward osmosis applications, *Journal of Membrane Science* 364 (2010) 233–241.
- [6] M. L. Stone, C. Rae, F. F. Stewart, A. D. Wilson, *Desalination* 312 (2013) 124–129.
- [7] P. G. Jessop, L. Kozycz, Z. Ghoshouni Rahami, D. Schoenmakers, A. R. Boyd, D. Wechsler, and A. M. Holland, Tertiary Amine Solvents having Switchable Hydrophilicity, *Green Chem.* 13 (2011) 619–623.
- [8] Mickley, 2008
- [9] M. L. Stone, C. Rae, F. F. Stewart, A. D. Wilson, *Desalination* 312 (2013) 124–129.
- [10] D. Wendt, B. Adhikari, C. Orme, A. Wilson, Produced Water Treatment Using the Switchable Polarity Solvent Forward Osmosis (SPS FO) Desalination Process: Preliminary Engineering Design Basis, GRC, 2016.
- [11] <http://www.multibriefs.com/briefs/cb-thermo/evaporative-technologies-for-recycling-produced-waters.pdf>.
- [12] <http://www.powerengineeringint.com/articles/print/volume-25/issue-2/features/solutions-for-coal-plant-wastewater-treatment.html>